

# *In situ* fast ellipsometric analysis of repetitive surface phenomena

J. Costa,<sup>a)</sup> J. Campmany,<sup>b)</sup> A. Canillas, J. L. Andújar, and E. Bertran

*Departament de Física Aplicada i Electrònica, Universitat de Barcelona, Av. Diagonal, 647, E08028 Barcelona, Catalonia (Spain)*

(Received 3 December 1996; accepted for publication 29 April 1997)

We present an ellipsometric technique and ellipsometric analysis of repetitive phenomena, based on the experimental arrangement of conventional phase modulated ellipsometers (PME) conceived to study fast surface phenomena in repetitive processes such as periodic and triggered experiments. Phase modulated ellipsometry is a highly sensitive surface characterization technique that is widely used in the real-time study of several processes such as thin film deposition and etching. However, fast transient phenomena cannot be analyzed with this technique because precision requirements limit the data acquisition rate to about 25 Hz. The presented new ellipsometric method allows the study of fast transient phenomena in repetitive processes with a time resolution that is mainly limited by the data acquisition system. As an example, we apply this new method to the study of surface changes during plasma enhanced chemical vapor deposition of amorphous silicon in a modulated radio frequency discharge of SiH<sub>4</sub>. This study has revealed the evolution of the optical parameters of the film on the millisecond scale during the plasma on and off periods. The presented ellipsometric method extends the capabilities of PME arrangements and permits the analysis of fast surface phenomena that conventional PME cannot achieve. © 1997 American Institute of Physics. [S0034-6748(97)00508-X]

## I. INTRODUCTION

The study of transient phenomena in surface processes is a subject of increasing interest in materials science, particularly in thin film technology where the analysis of the first stages of film growth is necessary to determine the film-substrate interface characteristics and the structural properties of the film.

Surface analytical techniques such as x-ray photoelectron spectroscopy, scanning electron microscopy, auger electron spectroscopy, or secondary ion mass spectrometry cannot be applied *in situ* to study processes such as chemical vapor deposition (CVD), etching, or corrosion, because of their ultrahigh vacuum requirements or because they are destructive. However, nondestructive optical techniques such as transmittance, reflectance, or ellipsometry are suitable for processes of these kinds, since they can operate in adverse environments such as reactive gases or plasmas.<sup>1</sup> Besides high sensitivity, ellipsometry can be used in real-time measurements.<sup>2,3</sup>

Phase modulated ellipsometry (PME) is suitable for the analysis of the kinetics of surface processes due to its relatively high speed.<sup>4</sup> In particular, it has been applied successfully to the real-time study of film growth kinetics, the nucleation and coalescence mechanisms, and the evolution of surface roughness.<sup>5,6</sup>

Even though the maximum theoretical acquisition rate of real-time PME is 1 kHz, when it works at this rate it loses precision. As shown in Fig. 1, a maximum acquisition rate of 25 Hz is needed to work with a precision of the measured

ellipsometric angles of better than 0.2°. Therefore, the time resolution standard of phase modulated ellipsometers is around 40 ms. The total integration time depends on the working frequency of the phase modulator (usually 50 kHz) and on the number of cycles needed to calculate the fast Fourier transformation (FFT) with reasonable precision (hundreds of cycles). Furthermore, the integration of the signal is also needed to eliminate noise from the light source (usually a Xe arc lamp) and the photomultiplier tube, and to eliminate the electrical noise associated with the analog-to-digital converter (ADC). Therefore, accurate measurement of fast transient processes with time constant of less than 40 ms by the conventional real-time PME technique does not seem to be possible at the present time.

Recently, there has been an increasing interest in the surface processes that involve transient phenomena faster than the conventional PME time resolution, such as film deposition or etching under a modulated discharge<sup>7</sup> or surface treatment by laser pulses.<sup>8</sup> Here we propose an alternative ellipsometric method based on a PME arrangement which is able to analyze the fast transient phenomena in repetitive surface processes. Periodic and triggered phenomena are repetitive processes often encountered in materials surface science.

In order to measure the transient behavior of the optical parameters of the sample, it is necessary to determine the reflected light polarization ellipse at each instant. With the proposed method, which we call the ellipsometric analysis of repetitive phenomena, the polarization ellipse is calculated *a posteriori* from the combination of three acquisitions of reflected light using three different configurations of the PME optical elements (modulator, polarizer, and analyzer). As a consequence of this procedure, a great improvement in the time resolution of the experimental data is achieved since the Fourier analysis of the signal detected is no longer necessary.

<sup>a)</sup>Also at: GRM: Grup de Recerca en Materials, Departament d'Enginyeria Industrial, Universitat de Girona, Av. Lluís Santaló s/n, E17071 Girona, Catalonia (Spain); Electronic mail: Josepcb@el.udg.es

<sup>b)</sup>Also at: Laboratori del Síncrotró de Barcelona, IFAE, Edifici Cn, UAB, Campus Universitari, E08193 Bellaterra, Catalonia (Spain).

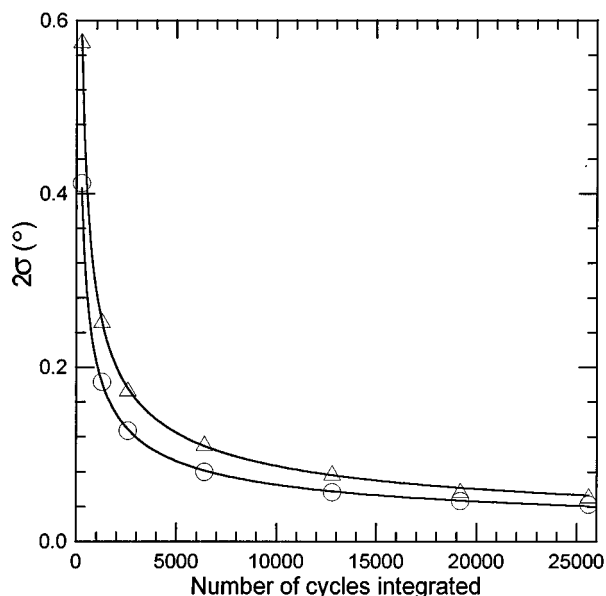


FIG. 1. Precision vs number of integrations for a standard PME operating in real-time mode. The precision is measured by  $2\sigma$ , the interval where 95% of experimental points lie, where  $\sigma$  is the standard deviation. Triangles correspond to the precision in the ellipsometric angle  $\Delta$  and circles to the ellipsometric angle  $\Psi$ . The frequency of the modulator (50 kHz) gives a period of each cycle of  $20 \mu\text{s}$ . A precision of  $0.2^\circ$  is reached by integrating 2000 cycles, giving an acquisition rate of 25 Hz operating in real-time mode.

Moreover, the signal-to-noise ratio is lower than that obtained by conventional PME measurements because the modulator does not operate and the flash type ADC is replaced by a successive approximation type ADC. Furthermore, calibration is performed as in the conventional PME.

In order to illustrate the performance of this method, we have applied it to the study of the transient variations of the reflection coefficient on the surface of an amorphous silicon film growing in a square wave modulated (SQWM) radio frequency  $\text{SiH}_4$  plasma.<sup>9,10</sup> In this case, it was possible to distinguish the changes in the ellipsometric angles,  $\Psi$  and  $\Delta$ , with a time resolution of better than 1 ms, which cannot be resolved by the conventional real-time PME method.

The combination of the phase modulated ellipsometry and the ellipsometric analysis of the repetitive phenomena method facilitates the expansion of the conventional PME to the study of new phenomena.

## II. THEORY

Figure 2 shows a schematic arrangement of a standard phase modulated ellipsometer (PME), where a light beam, coming from a Xe arc lamp, passes through a polarizer and a modulator before being reflected off the surface of the sample. After that, the light is analyzed by another polarizer, then dispersed by a monochromator, and finally detected by a photomultiplier tube.<sup>11</sup>

The ellipsometric analysis of the repetitive phenomena uses the same optical arrangement, and does not require the addition of any extra optical elements. This new method does not require the modulator to be operating. However, in order to make the use of this technique compatible with the conventional PME, the modulator is not removed.

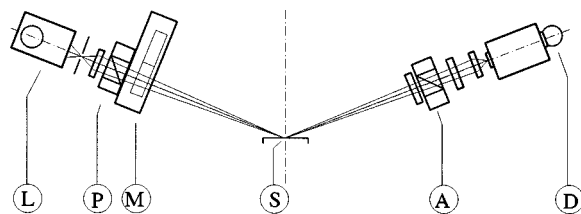


FIG. 2. Schematic arrangement diagram of the phase modulated ellipsometer elements: (P) Polarizer, (M) modulator, (S) sample, (A) analyzer, (L) Xe lamp, and (D) light detection system. Angles are taken positive in a counterclockwise sense when one is looking against the direction of propagation of the beam. The sample surface determines the plane of incidence;  $x$  direction perpendicular to the plane of incidence;  $y$ , direction parallel to the plane of incidence.

In order to calculate the ellipsometric angles,  $\Psi$  and  $\Delta$ , corresponding to the reflection on the sample, we use the Jones' matrix notation. In what follows, we describe the matrices of each element assuming specular surfaces and ideal polarizers.

The optical elements such as a polarizer, modulator, and analyzer can be mathematically described by the matrices  $\mathbf{P}$ ,  $\mathbf{M}$ , and  $\mathbf{A}$ , respectively, where

$$\mathbf{P} = \begin{pmatrix} 1 & 0 \\ 0 & 0 \end{pmatrix}, \quad \mathbf{M} = \begin{pmatrix} 1 & 0 \\ 0 & e^{j\delta_0} \end{pmatrix}, \quad \mathbf{A} = \begin{pmatrix} 1 & 0 \\ 0 & 0 \end{pmatrix}, \quad (1)$$

and  $\delta_0$  is the static phase shift introduced by the modulator in static conditions (power off).

The sample can be described by the matrix  $\mathbf{S}$ :

$$\mathbf{S} = \begin{pmatrix} \mathbf{r}_p & 0 \\ 0 & \mathbf{r}_s \end{pmatrix}, \quad (2)$$

where  $\mathbf{r}_p$  and  $\mathbf{r}_s$  are the complex reflection coefficients corresponding to the directions parallel and perpendicular to the incidence plane (Fig. 2), respectively. The complex ratio  $\rho$  between these coefficients can be expressed as a function of the ellipsometric angles  $\Psi$  and  $\Delta$  by

$$\rho = \frac{\mathbf{r}_p}{\mathbf{r}_s} = \tan \psi e^{j\Delta}. \quad (3)$$

Finally, the matrix  $\mathbf{R}(\alpha)$  describing a rotation by an angle  $\alpha$  of the optical axes with respect to the coordinate axes is given by

$$\mathbf{R}(\alpha) = \begin{pmatrix} \cos \alpha & \sin \alpha \\ -\sin \alpha & \cos \alpha \end{pmatrix}. \quad (4)$$

Once the matrices of the optical elements are established, the electric field  $E_{\text{PMA}}^t$  transmitted through the optical system shown in Fig. 2 is related to the incident electric field  $E^i$  by:

$$E_{\text{PMA}}^t = \mathbf{A}\mathbf{R}(\alpha)\mathbf{S}\mathbf{R}(\alpha)\mathbf{M}\mathbf{R}(\alpha)\mathbf{P}E^i, \quad (5)$$

where  $\mathbf{A}$ ,  $\mathbf{P}$ , and  $\mathbf{M}$  represent the angles between the plane of incidence and the analyzer, polarizer, and modulator, respectively.

Developing the above equation, we obtain the following expression for  $E_{\text{PMA}}^t$ :

$$E_{\text{PMA}}^t = \{[\mathbf{r}_p \cos A \cos M - \mathbf{r}_s \sin A \sin M] \cos(P - M) - [\mathbf{r}_p \cos A \sin M + \mathbf{r}_s \sin A \cos M] e^{i\delta_0} \times \sin(P - M)\} E^i. \quad (6)$$

This is the basic expression for the electric field detected corresponding to a PME configuration with a nonoperating phase modulator, i.e.,  $\delta_0$  constant.

Equation (6) can be simplified by performing the measurements with an angle  $P - M = 0$ . Then, the static birefringence  $\delta_0$  introduced by the nonoperating modulator is eliminated:

$$E_{\text{PMA}}^t = (\mathbf{r}_p \cos A \cos M - \mathbf{r}_s \sin A \sin M) E^i. \quad (7)$$

The measured intensity in the photomultiplier tube, for a given angular configuration,  $\mathbf{I}_{\text{PMA}}$ , can be expressed as

$$\mathbf{I}_{\text{PMA}} = k E_{\text{PMA}}^t E_{\text{PMA}}^{t*}, \quad (8)$$

where  $E_{\text{PMA}}^{t*}$  is the conjugated complex of  $E_{\text{PMA}}^t$  and  $k$  is the responsivity of the photomultiplier tube. Expanding Eq. (8) according to Eq. (7), we obtain

$$\mathbf{I}_{\text{PMA}} = (\mathbf{r}_s^2 \sin^2 A \sin^2 M + \mathbf{r}_p^2 \cos^2 A \cos^2 M - (\mathbf{r}_s^* \mathbf{r}_p + \mathbf{r}_s \mathbf{r}_p^*) \sin A \cos A \sin M \cos M) k^2 E^i. \quad (9)$$

As we can observe, there are three unknowns:  $k^2 - E^i$ ,  $\mathbf{r}_s$ , and  $\mathbf{r}_p$ . Only three independent measurements at different angle configurations are needed to determine their values. With the experimental arrangement shown in Fig. 2, we must perform these three measurements of light intensity nonsimultaneously, in order to change the angular configurations. The repetitivity of the surface process should guarantee that in these three measurements we are monitoring the same phenomenon. Provided that this condition is satisfied, the ellipsometric analysis of the repetitive phenomena method permits us to average the experimental points of one of these acquisitions over the number of periods necessary to obtain good precision.

Measurements can be performed in several sets of configurations. The criteria to chose a particular set of configurations are the minimization of the associated error of the measured  $\Psi$  and  $\Delta$ , the minimization of the mechanical changes in optical elements, and the simplicity of the equation (elimination of  $\delta_0$ ).

We can take multiple values of angles that simplify Eq. (9). A suitable set of angles can be  $P - M = 0$ ,  $M = \pi/4$  and  $A = \pi/4$ ,  $-\pi/4$  and  $\pi/2$ . For this set of angles (Set I), in each measurement only the azimuth of the analyzer has been changed. The advantage of this choice is the possibility of easy automatization of measurements by means of an automatized analyzer. For this configuration, we have, respectively,

$$\mathbf{I}_{0,\pi/4,\pi/4} = [\mathbf{r}_p^2 + \mathbf{r}_s^2 - (\mathbf{r}_s^* \mathbf{r}_p + \mathbf{r}_s \mathbf{r}_p^*)] \frac{E^i k^2}{4}, \quad (10)$$

$$\mathbf{I}_{0,\pi/4,-\pi/4} = [\mathbf{r}_p^2 + \mathbf{r}_s^2 + (\mathbf{r}_s^* \mathbf{r}_p + \mathbf{r}_s \mathbf{r}_p^*)] \frac{E^i k^2}{4}, \quad (11)$$

$$\mathbf{I}_{0,\pi/4,\pi/2} = \frac{1}{2} \mathbf{r}_s^2 E^i k^2. \quad (12)$$

Arranging the above expressions, we finally obtain

$$\tan^2 \psi = \frac{\mathbf{I}_{0,\pi/4,\pi/4} + \mathbf{I}_{0,\pi/4,-\pi/4} - \mathbf{I}_{0,\pi/4,\pi/2}}{\mathbf{I}_{0,\pi/4,\pi/2}}, \quad (13)$$

$$\tan \psi \cos \Delta = \frac{\mathbf{I}_{0,\pi/4,-\pi/4} - \mathbf{I}_{0,\pi/4,\pi/4}}{2\mathbf{I}_{0,\pi/4,\pi/2}}. \quad (14)$$

So, we can obtain the ellipsometric angles  $\Psi$  and  $\Delta$  by performing three measurements, each one using a different configuration for every run.

Another possibility of ellipsometric analysis or repetitive phenomena is the measurement of the phase modulator static birefringence  $\delta_0$ . This could be done by setting  $P - M = \pm \pi/4$  in Eq. (6) and operating the ellipsometric arrangement with  $M = 0$  and  $A = 3\pi/4$ ,  $\pi/4$ , and  $\pi/2$  (Set II). Combining the measured intensities, as was done in Eqs. (13) and (14), yields:

$$\tan^2 \Psi = \frac{\mathbf{I}_{\pi/4,0,\pi/4} + \mathbf{I}_{\pi/4,0,3\pi/4} - \mathbf{I}_{\pi/4,0,\pi/2}}{\mathbf{I}_{\pi/4,0,\pi/2}}, \quad (15)$$

$$\tan \psi \cos \Delta' = \frac{\mathbf{I}_{\pi/4,0,3\pi/4} - \mathbf{I}_{\pi/4,0,\pi/4}}{2\mathbf{I}_{\pi/4,0,\pi/2}}, \quad (16)$$

where  $\Delta' = \Delta + \delta_0$ .

Therefore, performing the measurements with the angular configurations specified in Sets I and II, it is possible to deduce the value of  $\delta_0$ .

### III. EXPERIMENT

In order to illustrate the possibilities of this method, the ellipsometric analysis of repetitive phenomena has been applied to the study of the growth of a hydrogenated amorphous silicon thin film (*a*-Si:H) in a modulated discharge. The deposition system was a capacitively coupled plasma rf reactor described elsewhere,<sup>11</sup> which is provided with a conventional phase modulated ellipsometer.<sup>12</sup> The deposition conditions were 30 Pa of pressure, 300 °C of substrate temperature, and a flow rate of 30 sccm of SiH<sub>4</sub>. The rf power was modulated between 0 and 80 W by controlling the rf power source with a conventional function generator (OR-X 402). The modulation signal was a square wave, its frequency was 13 Hz and its duty cycle 50%. Ellipsometric analysis of repetitive phenomena measurements were performed with the PME arrangement using Set I because it avoids the calibration of  $\delta_0$ .

Measurements were taken with a standard acquisition card (PCLAB 718) at a data measurement rate of 65 kHz. In order to reduce the noise associated with the detection, we chose a successive approximation 12-bit ADC device. The acquisition card is controlled by a personal computer that calculates the average of several plasma modulation cycles.

The data for each angle configuration were acquired by averaging the signal over 256 plasma modulation cycles. The time between experimental points was 16  $\mu$ s. The acquisition was triggered by the plasma modulation signal. The photomultiplier tube was maintained at a constant bias of 900 V.

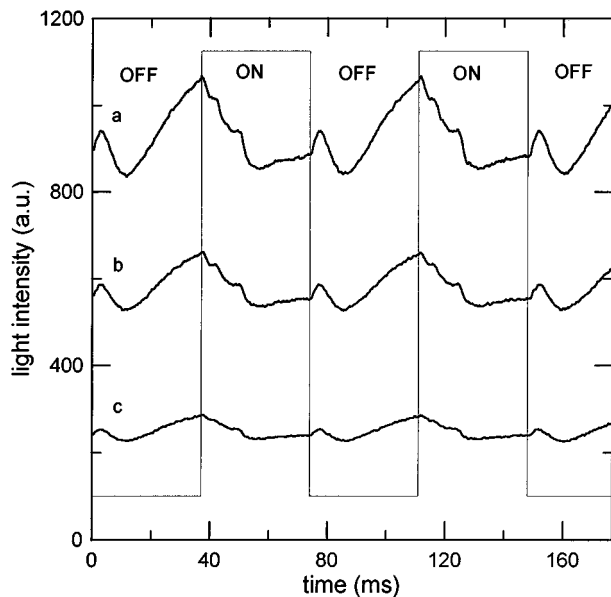


FIG. 3. Intensities obtained by ellipsometric analysis or repetitive phenomena. Using the notation defined in the text, curve (a) corresponds to the intensity  $I_{0,\pi/4,\pi/4}$ , and curve (b) to  $I_{0,\pi/4,-\pi/4}$ , and curve (c) to  $I_{0,\pi/4,\pi/2}$ . The square wave corresponds to the plasma modulation signal.

The light intensities from the plasma emission and background were subtracted from the measured intensities of the reflected light beam. We also checked that the electric plasma switching on and off had no influence on the ellipsometric measurements, so all changes observed in reflected light can be attributed to changes in the surface or bulk structural properties.

Measurements were performed with an angle of incidence of the light beam of  $69^{\circ}50'$  and at a wavelength of 340 nm. This wavelength was chosen to monitor only the surface properties, because it is near the maximum of the absorption of *a*-Si:H. The angles of polarizers were calibrated with conventional PME.

Ellipsometric analysis of repetitive phenomena measurements were performed 10 min after starting the modulated discharge. At this time, the optical parameters of the growing *a*-Si:H film reached a steady state, as shown by monitoring with conventional PME.<sup>9</sup> However, as the next section demonstrates, the ellipsometric analysis of the repetitive phenomena method was able to resolve the evolution of the ellipsometric angles within a period of plasma modulation. The analysis of the film surface at this quasisteady state guarantees that each acquisition at each angular configuration observes the same phenomena.

#### IV. RESULTS AND DISCUSSION

Figure 3 shows the modulation signal and the reflected light intensities,  $I_{PMA}$ , obtained at the three angular configurations that were specified as Set I. The interval of plasma on shows a decrease in the reflected light intensity, overlapped to small evolutions, followed by a weak and monotonic increase in the intensity. When the plasma is turned off, there is an initial intensity peak (just in the afterglow), after which

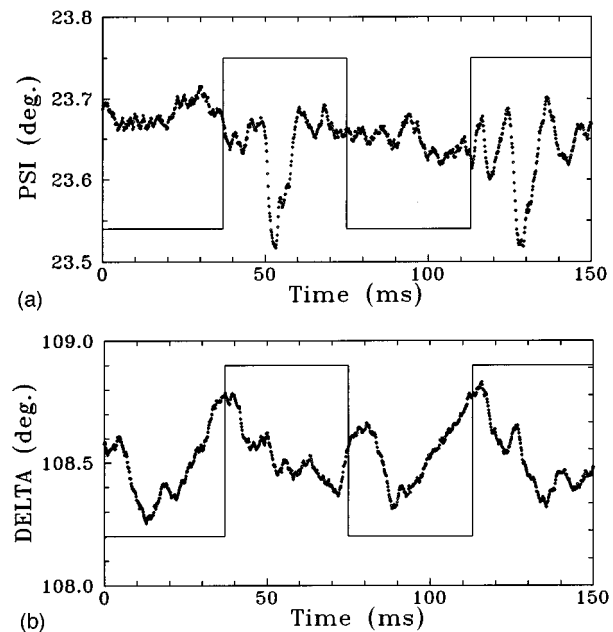


FIG. 4. (a) Values of  $\Psi$  calculated from intensities shown in Fig. 3. (b) Values of  $\Delta$  calculated from intensities shown in Fig. 3. The square wave corresponds in both cases to the plasma modulation signal.

the reflected intensity increases. This increase continues until the plasma starts again. These features were completely repetitive over the entire experiment time.

Figure 4 shows the consequent variation of the ellipsometric angles  $\Psi$  and  $\Delta$  calculated from the above mentioned intensities using Eqs. (13) and (14). Both angles, demonstrated a significant evolution during the modulation cycle. The most relevant feature of angle  $\Psi$  is that it shows a peak around 15 ms after the plasma starts. On the other hand, angle  $\Delta$  evolves more monotonically: decreasing  $\Delta$  during plasma on and increasing during plasma off.

In order to model the evolution of the ellipsometric angles in terms of the film microstructure, we have to take into account the complexity of the processes involved during film growth. The deposition rate of the *a*-Si:H film is around  $10 \text{ \AA/s}$  for the deposition conditions used in the present experiment and so, in a modulation period of 13 Hz the film thickness has increased  $0.8 \text{ \AA}$ . Therefore, the variations observed in the ellipsometric angles during a modulation period (see Fig. 4) correspond to the combined result of the species incorporation along with surface processes at the submonolayer scale. This makes it impossible to model the film evolution using simple standard assumptions, for example, surface roughness increase, nucleation, and coalescence. However some trends of the  $\Psi$  and  $\Delta$  evolutions can be interpreted on the basis of ellipsometric studies dealing with the initial transients of silane discharges after its ignition<sup>9,13,14</sup> and the contribution of species from the plasma (neutrals and ionized). After the plasma ignition, the deposition of a less dense *a*-Si:H material has been suggested.<sup>13,14</sup> This deposition can account for the sudden variation observed for the  $\Psi$  angle during the on period, 10 ms after the

ignition. On the other hand, a constant value of  $\Psi$  and a decrease in  $\Delta$  with time may indicate a slight increase in surface roughness.

The variations of the  $\Delta$  angle during the off period could be interpreted on the basis of the incorporation of negative ions, powder particles, and clusters, that are generated and electrostatically confined by the plasma sheaths during plasma on.<sup>15</sup> When the rf power is switched off, the plasma potential sheath disappears and all the above species are allowed to reach the layer. Thus, the decrease of the  $\Delta$  angle during the first 15 ms could be attributed to this fact. On the other hand, during the rest of the time, the surface diffusion, chemical binding, and other atomic processes at the surface may be responsible for the compactation of the film that results in a return of  $\Delta$  to its initial value.

Finally, these results illustrate that the presented technique (ellipsometric analysis of repetitive phenomena) is suitable to study the surface phenomena that require a great improvement in time resolution and it opens new capabilities to conventional PME arrangements.

## ACKNOWLEDGMENT

This work was supported by the CICYT of Spain under Contract No. MAT96-1194-C02-01.

- <sup>1</sup>R. W. Collins and Y. T. Kim, *Anal. Chem.* **62**, 887A (1990).
- <sup>2</sup>I. An, Y. M. Li, H. V. Nguyen, and R. W. Collins, *Rev. Sci. Instrum.* **63**, 3842 (1992).
- <sup>3</sup>M. Kildemo and B. Drévilion, *Rev. Sci. Instrum.* **67**, 1956 (1996).
- <sup>4</sup>B. Drévilion, J. Y. Parey, M. Stchakovsky, R. Benferhat, Y. Josserand, and B. Schlayen, *Proc. SPIE* **1188**, 174 (1989).
- <sup>5</sup>A. Canillas, E. Bertran, J. L. Andújar, and B. Drévilion, *J. Appl. Phys.* **68**, 2752 (1990).
- <sup>6</sup>B. Drévilion, *Prog. Cryst. Growth Charact. Mater.* **27**, 1 (1993).
- <sup>7</sup>L. L. Overzet, J. H. Beberman, and J. T. Verdeyen, *J. Appl. Phys.* **66**, 1622 (1989).
- <sup>8</sup>P. M. Fauchet and I. H. Campbell, *J. Non-Cryst. Solids* **137**, 729 (1991).
- <sup>9</sup>A. Lloret, E. Bertran, J. L. Andújar, A. Canillas, and J. L. Morenza, *J. Appl. Phys.* **69**, 632 (1991).
- <sup>10</sup>J. L. Andújar, A. Canillas, J. Campmany, E. Bertran, J. Serra, C. Roch, and A. Lloret, *J. Appl. Phys.* **71**, 1546 (1992).
- <sup>11</sup>A. Canillas, E. Bertran, J. L. Andújar, and J. L. Morenza, *Vacuum* **39**, 785 (1989).
- <sup>12</sup>J. L. Andújar, E. Bertran, A. Canillas, J. Esteve, J. Andreu, and J. L. Morenza, *Vacuum* **39**, 795 (1989).
- <sup>13</sup>R. W. Collins and A. Pawlowski, *J. Appl. Phys.* **59**, 1160 (1986).
- <sup>14</sup>U. I. Schmidt, B. Schröder, and H. Oechsner, *Thin Solid Films* **233**, 297 (1993).
- <sup>15</sup>J. T. Verdeyen, J. H. Beberman, and L. J. Overzet, *J. Vac. Sci. Technol. A* **8**, 1851 (1990).